Studies of RNA Cleavage by Photolysis of *N*-Hydroxypyridine-2(1*H*)-thione. A New Photochemical Footprinting Method†

Steven G. Chaulk, John Paul Pezacki, and Andrew M. MacMillan*

Department of Chemistry, University of Toronto, 80 St. George Street, Toronto, Ontario, Canada M5S 3HG

Received April 21, 2000; Revised Manuscript Received June 15, 2000

ABSTRACT: *N*-Hydroxypyridine-2(1*H*)-thione (N-HPT) has been studied as a photochemical source of hydroxyl radicals for use in photoinitiated nucleic acid footprinting experiments. Steady-state photolysis of dilute aqueous solutions of N-HPT at 350 nm in the presence of a 385 nucleotide ^{32}P-labeled RNA, the *Tetrahymena* L-21 ribozyme, resulted in cleavage of the RNA at nucleotide resolution. No cleavage of the RNA occurred in the absence of light or in the absence of N-HPT. Photolysis of the analogous pyridine lacking the *N*-hydroxyl group did not result in detectable amounts of RNA cleavage. The addition of RNA to preirradiated solutions of N-HPT gave no apparent RNA cleavage products, suggesting that the photoproducts of N-HPT do not result in RNA modification. Cleavage of RNA, upon photolysis in the presence of N-HPT, occurred in a sequence-independent fashion with double-stranded RNA being cleaved as efficiently as single-stranded RNA. Based on these observations, we conclude that photochemically generated diffusable hydroxyl radicals are responsible for the RNA cleavage. Experiments involving the photolysis of N-HPT in the presence of the *Tetrahymena* ribozyme and magnesium showed a magnesium-dependent protection from RNA cleavage due to formation of a folded RNA tertiary structure. The locations and amount of protection were identical to those observed in footprinting experiments performed with other hydroxyl radical sources. The presence of N-HPT had no effect on either the rate of folding or the catalytic activity of the folded RNA, indicating that this reagent does not disrupt RNA tertiary structure or otherwise affect activity. Thus, N-HPT is established as a new reagent for use in photoinitiated RNA footprinting experiments.

Hydroxyl radicals are important reactive species which have been widely used in studies of higher order nucleic acid structure and complexes formed between small molecules or proteins and nucleic acids (*1, 2*). Initial hydrogen abstraction from the ribose or the deoxyribose moiety is followed by a reaction cascade which results in cleavage of the phosphodiester backbone. Sequence-independent cleavage of both single-stranded and double-stranded DNA and RNA molecules can be analyzed at nucleotide resolution by denaturing polyacrylamide gel electrophoresis (PAGE)[1] of ^{32}P-labeled molecules. The formation of either higher order structure or specific complexes can lead to protection from such cleavage. A region of reduced cleavage, usually detected by denaturing PAGE, is referred to as a footprint. Footprinting experiments have typically been used to provide structural information on systems at equilibrium. When it is possible to measure footprints as a function of time, it then becomes possible to make inferences about rates and mechanisms of dynamic processes of which RNA folding is one example.

Common sources of hydroxyl radicals in footprinting experiments include the copper-phenanthroline and iron-EDTA (Fenton's reagent) transition metal complexes formed with Cu^{2+} and Fe^{2+}, respectively (*1*−*3*). In the presence of hydrogen peroxide and a reducing agent, hydroxyl radicals are produced from such complexes in sufficient quantity to effect DNA or RNA cleavage (*1*−*5*). Synchroton X-ray irradiation of water can be used to produce hydroxyl radicals on a millisecond time scale (*6*). Radicals produced in such a fashion have been used to footprint the *lac* repressor−DNA complex (*7*). As well, X-ray-generated radicals were used to perform time-resolved or kinetic footprinting studies. In an elegant series of experiments, Chance, Brenowitz, and Woodson were able to analyze the magnesium-dependent folding pathway of the 385 nucleotide *Tetrahymena* L-21 ribozyme (*8*). Recently, we have shown that peroxynitrous acid can also be used as a kinetic footprinting reagent, allowing analysis of dynamic processes occurring with half-lives of greater than ∼3 s (*9, 10*). Our interest in the dynamics of several RNA systems has led us to consider the possibility of employing photochemical methods as a means of conducting nucleic acid footprinting experiments.

Although there have been a number of reports of photochemically induced cleavage of RNA and DNA involving both oxidative and hydrolytic cleavage pathways (*11*), only hydrogen peroxide has been successfully used to photochemically footprint DNA using near molar concentrations of H_2O_2 (*12*). As far as we are aware, no other compounds

† This work was supported by the Natural Sciences and Engineering Research Council of Canada (NSERC). S.G.C. is the recipient of a Walter C. Sumner Fellowship, and J.P.P. was supported by an NSERC postdoctoral fellowship.

* To whom correspondence should be addressed. Tel/FAX: 416-978-8603; e-mail: amacmill@chem.utoronto.ca.

[1] Abbreviations: 2-MP, 2-mercaptopyridine; N-HP, *N*-hydroxypyridine-2(1*H*)-one; N-HPT, *N*-hydroxypyridine-2(1*H*)-thione; PAGE, polyacrylamide gel electrophoresis.

10.1021/bi0009136 CCC: $19.00
Published on Web 08/03/2000

have been established as DNA or RNA photochemical footprinting reagents. Some advantages of photochemical footprinting reagents are the following: they allow premixing of all components of the footprinting reaction prior to irradiation; they allow for the precise control of the cleavage conditions by light; and they have potential for use in kinetic experiments such as time-resolved probing of nucleic acid structure.

One common feature of organic or organometallic reagents that affects photochemical cleavage of nucleic acids is that they often bind and interact with DNA and RNA (*11*). Such interactions may alter the photochemistry of the precursor and perturb the structure of the DNA or RNA; in addition, sequence-specific binding to the polynucleotide results in sequence-specific cleavage upon photolysis. For example, irradiation of rhodium(II) complexes bound to DNA results in strand cleavage with observed products consistent with a sequence-specific radical-based cleavage pathway (*13*−*16*). Cobalt(III)−bleomycin complexes can also cleave DNA photochemically in a sequence-selective manner (*17*, *18*). These complexes are thus very useful as sequence-specific probes of DNA. However, they have limited utility as footprinting reagents because of the requirement for sequence-independent cleavage in such experiments.

Several classes of organic compounds can act as photochemical sources of hydroxyl radicals (so-called photo-Fenton reagents). Examples include alkylperoxides such as **1** (*19*) that undergo bond homolysis upon photolysis, yielding an alkoxyl radical and a hydroxyl radical (although these reactions may be more complex; *20*), *N*-oxides such as **2** (*21*), and *N*-hydroxypyridines such as *N*-hydroxypyridine-2(1*H*)-one (N-HP) (*22*) and *N*-hydroxypyridine-2(1*H*)-thione (N-HPT) (*23*) that undergo N−O bond homolysis (eq 1). Little is known about either the interactions of these compounds with nucleic acids or the chemistry resulting from their irradiation in the presence of nucleic acids. In the present study, we chose to investigate photochemical cleavage reactions utilizing N-HPT because it can be irradiated with ≥350 nm light with negligible light-induced RNA degradation occurring after prolonged exposures.

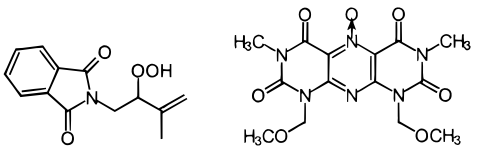

N-HPT (N-HP) (1)

Redmond and co-workers have performed detailed photochemical investigations of several *N*-hydroxypyridinethiones and *N*-hydroxypyridinones, including N-HP and N-HPT (Scheme 1), that generate hydroxyl radicals in buffered aqueous solutions with reasonable quantum yields (*22*−*24*).

In addition, it has been shown that oxidative damage of DNA, consistent with production of hydroxyl radicals, is observed with N-HPT (*25*). Here we report studies of the photolysis of N-HPT in the presence of RNA (eq 2):

Scheme 1

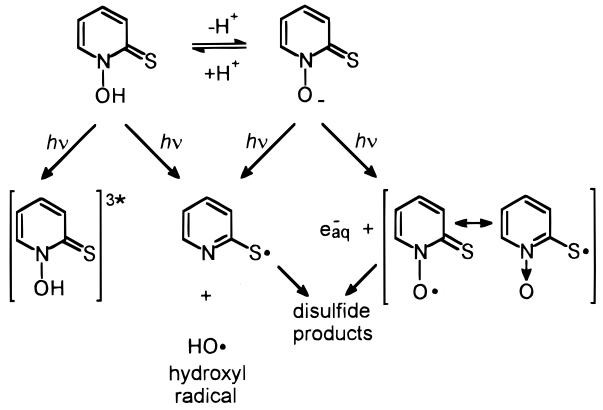

$$\text{N-HPT} \xrightarrow{h\nu} \text{HO}\cdot \xrightarrow{\text{RNA}} \text{RNA cleavage products} \quad (2)$$

which result in nonselective RNA cleavage in experiments using the *Tetrahymena* ribozyme as a model system. N-HPT does not interfere with the folding kinetics of the *Tetrahymena* ribozyme nor does it affect the activity of the folded ribozyme. These experiments establish N-HPT as a new photochemical footprinting reagent.

MATERIALS AND METHODS

N-Hydroxypyridine-2(1*H*)-thione and 2-mercaptopyridine were obtained from Aldrich. The pT7L-21 plasmid was provided by Dr. Jamie Williamson (Scripps Research Institute). *Sca*I restriction enzyme, nucleoside triphosphates, and ribonuclease inhibitor were from Pharamacia, T7 RNA polymerase was from Promega, calf intestinal alkaline phosphatase was from Boehringer Manheim, and T4 polynucleotide kinase was from New England Biolabs. The 11 nucleotide L-21 *Sca*I substrate, CCCUCUAAAAA, was obtained from Cruachem. [γ-^{32}P]ATP (6000 Ci/mmol, 5 mCi/0.03 mL) was purchased from New England Nuclear. Quiksep spin columns were purchased from Isolab Inc.

Steady-State Photolysis. Steady-state photolyses were carried out in a Rayonet photochemical reactor equipped with 8−12 350 nm lamps which provided ∼12 mW/cm^2 light. Samples were prepared in either Pyrex or quartz vessels. Experiments involving photolyses of RNA samples were performed in 5 mm Pyrex NMR tubes that had been cut to ∼2 cm in length. Samples were positioned on a rack and photolyzed at 350 nm in a Rayonet reactor. All samples from a given set of experiments were photolyzed simultaneously under identical conditions.

Preparation of RNA. The pT7L-21 plasmid was digested for runoff transcription. Digestion reactions (200 μL) contained pT7L-21 plasmid (20 μg), *Sca*I (200 units), 70 mM Tris, pH 7.6, 10 mM $MgCl_2$, 5 mM DTT and proceeded for 10 h at 37 °C. Reactions were then extracted with phenol/chloroform/isoamyl alcohol and chloroform/isoamyl alcohol and ethanol precipitated. Transcriptions (0.5 mL) were performed for 6 h at 37 °C in 40 mM Tris (pH 8), 6 mM $MgCl_2$, 2 μM spermidine, 10 mM NaCl, 10 mM DTT, using 1 mM nucleoside triphosphates, 20 units of ribonuclease inhibitor, 400 units of T7 RNA polymerase, and 10 μg *Sca*I-digested pT7L-21 plasmid as template. Transcriptions were

purified directly by denaturing 20% (19:1) PAGE. The transcript was visualized by UV shadowing, excised, and extracted with phenol/chloroform/isoamyl alcohol (200 μL) and 0.3 M NaOAc (pH 5.3, 400 μL) for 4 h at 37 °C. After extraction, polyacrylamide was removed by centrifugation through a paper-disk spin column. The filtrate was then extracted with chloroform/isoamyl alcohol and ethanol precipitated. RNA was resuspended in 50 μL of TE and stored at −78 °C to minimize degradation.

Ribozyme 5′-End-Labeling. L-21 Group I ribozyme (300 pmol) was 5′-dephosphorylated with 3 units of calf intestinal alkaline phosphatase for 20 min in 25 μL reactions at 37 °C containing 50 mM Tris-HCl, 0.1 mM EDTA, followed by an additional 3 units of CIAP for 20 min. Reactions were then extracted with phenol/chloroform/isoamyl alcohol and chloroform/isoamyl alcohol followed by ethanol precipitation. L-21 Group I ribozyme labeling reactions (40 μL) contained 150 pmol of RNA, 70 mM Tris, pH 7.6, 10 mM $MgCl_2$, 5 mM DTT, 4 units of T4 polynucleotide kinase, and 6 μL of [γ-^{32}P]ATP and proceeded for 15 min at 37 °C. Reactions were then purified directly by denaturing 4% (19:1) PAGE. The transcript was visualized by autoradiography, excised, and extracted with phenol/chloroform/isoamyl alcohol (200 μL) and 0.3 M NaOAc (pH 5.3, 200 μL) for 4 h at 37 °C. After extraction, polyacrylamide was removed by centrifugation through a paper-disk spin column; the filtrate was then extracted with chloroform/isoamyl alcohol and ethanol precipitated. RNA was resuspended in 50 μL of TE and stored at −78 °C to minimize degradation.

Endoribonuclease Activity Folding Assay. The rate of folding of the L-21 Group I ribozyme was assayed by its endoribonuclease activity (CCCUCUAAAAA + GTP → CCCUCU + pppGAAAAA) at 25 °C (*26*). Aliquots (10 μL) from a ribozyme stock solution (100 nM ribozyme, 80 mM NaCl, 10 mM $MgCl_2$, 50 mM NaH_2PO_4/Na_2HPO_4, pH 7) were combined with aliquots (10 μL, 1×10^5 cpm) of a substrate stock solution (32 nM 5′-end-labeled substrate, 80 mM NaCl, 10 mM $MgCl_2$, 50 mM NaH_2PO_4/Na_2HPO_4, pH 7, 1 mM GTP) at the indicated times (see Figures 2 and 3) following $MgCl_2$ addition to the ribozyme stock solution. Reactions proceeded for 30 s before being quenched with an equal volume of stop solution (100 mM Na_2EDTA, 6.4 M urea, 0.4 mg/mL bromophenol blue, 0.4 mg/mL xylene cyanole, 0.4 M Tris base, 0.4 M boric acid). Reactions were then subjected to denaturing 20% (19:1) PAGE for 2 h at 30 mA. Gels were exposed to a Molecular Dynamics Phosphor Screen which was then scanned on a Molecular Dynamics Storm 860 Phosphorimager. Extents of reaction were quantitated (ImageQuant 5.0), and a plot of normalized extent of reaction versus folding time was fitted to a first-order exponential (GraFit 3.00) using data from two experiments.

For the experiments with N-HPT, the ribozyme and substrate stock solutions were 1.0 mM in N-HPT.

Potassium Peroxynitrite Synthesis. To a stirring ice-cooled aqueous solution (10 mL) containing 0.6 M (0.41 g) $NaNO_2$ and 3% H_2O_2 was added 0.5 M HCl (5 mL) followed immediately by a solution (5 mL) containing 400 μM (3.3 mg) diethylenetriaminepentaacetic acid and 1.6 M KOH. The resulting mixture was stirred for 5 min. Then MnO_2 (100 mg) was added and stirring continued for 20 min. Excess MnO_2 was removed by centrifugation (performed at 4 °C). Typical yields of potassium peroxynitrite were 80−130 mM by UV absorbance at 302 nm ($\epsilon = 1670\ M^{-1}$). A delay of even several seconds in the addition of the KOH/diethylenetriaminepentaacetic acid solution resulted in significantly lower yields of potassium peroxynitrite. The potassium peroxynitrite solution was then stored at −78 °C with no decrease in concentration after 6 months.

Peroxynitrous Acid Footprinting. L-21 Group I ribozyme folding was initiated by the addition of $MgCl_2$ (final concentration 10 mM) to a solution (final volume 20 μL) containing final concentrations of 80 mM NaCl, 50 mM NaH_2PO_4/Na_2HPO_4 (pH 7), 50 nM 5′-end-labeled ribozyme (1.0×10^6 cpm) at 25 °C (*9*). Footprinting was then effected by the addition of potassium peroxynitrite (1 μL, 80−130 mM). Footprinting reactions were allowed to proceed for 20 s before freezing on dry ice, followed by ethanol precipitation. Reactions (1.0×10^6 cpm) were then subjected to denaturing 6% (19:1) PAGE at 85 W for 1.5 h. Dried gels were exposed to a Molecular Dynamics Phosphor Screen which was then scanned on a Molecular Dynamics Storm 860 Phosphorimager. To calculate the fractional peroxynitrous acid protection (footprint), background intensity (ImageQuant 5.0) was first subtracted and a correction for differences in lane loading applied. Then the intensity of a region in the "folded" lane was divided by the intensity of the same region in the "unfolded" lane to give the fractional protection.

Size Standards: RNase T1 Ladder. Positions of hydroxyl radical induced RNA cleavage were determined by comparison to an RNase T1 cleavage ladder. RNase T1 cleavage reactions were carried out by adding 2.5 units of RNase T1 (Pharmacia) to a solution (50 μL, pH 5.0, 55 °C) containing 18 mM citric acid, 0.9 mM Na_2EDTA, 6.3 M urea, 100 nM 5′-end-labeled ribozyme (7.5×10^6 cpm), and 13.5 mg/mL tRNA. Reactions proceeded for 1 min and were then extracted with phenol/chloroform/isoamyl alcohol, chloroform/isoamyl alcohol followed by ethanol precipitation. Approximately 2×10^5 cpm were loaded per lane.

Photoinitiated Cleavage with N-HPT. Solutions containing 50 nM ribozyme (1×10^6 cpm), 50 mM NaH_2PO_4/Na_2HPO_4 (pH 7), 0.1 mM EDTA, and 1 mM N-HTP or 1 mM 2-mercaptopyridine were placed in 5 mm Pyrex NMR tubes and photolyzed for 5 min at 350 nm in a Rayonet reactor. Following photolysis, reactions were ethanol precipitated and subjected to 6% PAGE at 85 W for 1.5 h. For the dark control reactions, the above solutions were kept at room temperature for 5 min before ethanol precipitation. Dried gels were exposed to a Molecular Dynamics Phosphor Screen which was then scanned on a Molecular Dynamics Storm 860 Phosphorimager.

RNA Footprinting with N-HPT. Solutions containing 50 nM ribozyme (1×10^6 cpm), 50 mM NaH_2PO_4/Na_2HPO_4 (pH 7), 0.1 mM EDTA, 1 mM N-HTP, and 10 mM $MgCl_2$ were incubated at room temperature for 10 min to allow folding of the RNA. Reactions were then placed in 5 mm Pyrex NMR tubes and photolyzed for 5 min at 350 nM in a Rayonet reactor. Following photolysis, reactions were ethanol precipitated and subjected to 6% PAGE at 85 W for 1.5 h. Dried gels were exposed to a Molecular Dynamics Phosphor Screen which was then scanned on a Molecular Dynamics Storm 860 Phosphorimager. Footprints were analyzed in the same fashion as those observed in the peroxynitrous acid experiments.

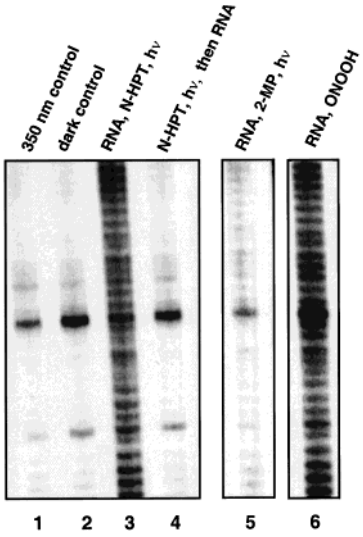

FIGURE 1: Denaturing PAGE analysis of unfolded, ^{32}P-labeled *Tetrahymena* L-21 RNA. Lane1: Photolysis (350 nm, 5 min) in the absence of N-HPT. Lane 2: N-HPT incubation (5 min) of ribozyme without photolysis. Lane 3: RNA cleavage from photolysis (350 nm, 5 min) of 1 mM N-HPT. Lane 4: RNA added after 1 mM N-HPT photolysis (350 nm, 5 min). Lane 5: Photolysis (350 nm, 5 min) of 2-MP (2-mercaptopyridine) in the presence of ribozyme. Lane 6: RNA cleavage using peroxynitrous acid.

RESULTS

Steady-State Photolysis of N-HP and N-HPT. We examined the steady-state photolysis of N-HPT in dilute and buffered aqueous solutions. Irradiation of dilute solutions of N-HPT (1 mM) buffered with phosphate to pH 7 was carried out using a Rayonet reactor equipped with 8−12 350 nm bulbs as the light source. Conversion was monitored by measuring the UV absorbance of the solutions and was found to be ∼73% after 1 min and complete after 5 min of irradiation. We also examined the 350 nm photolysis of *N*-hydroxy-2(1*H*)-pyridone (N-HP). However, significantly longer irradiation times were required for conversion of N-HP because it does not have a significant absorption at 350 nm. Studies using N-HP were not pursued further.

RNA Cleavage Initiated by Photolysis of N-HPT. We prepared the *Tetrahymena* intron RNA for cleavage studies by T7 transcription from the plasmid pT7L-21 followed by 5′-end-labeling with ^{32}P. The RNA was added to a pH 7 phosphate-buffered solution containing 1 mM N-HPT, and the solutions were irradiated at 350 nm for 5 min. Analysis of these samples by denaturing PAGE revealed cleavage of the RNA to smaller fragments (Figure 1, lane 3). The observed cleavage pattern strongly suggests that N-HPT does not exhibit sequence selectivity in the cleavage reaction. The percent cleavage of RNA is highly dependent on the concentration of N-HPT, and concentrations between 1 and 2 mM N-HPT were determined to be optimal for short irradiation times (1−5 min). RNA cleavage was dependent on both irradiation and the presence of the *N*-hydroxy group. Incubation of RNA in the dark with N-HPT or irradiation of samples containing 2-mercaptopyridine (2-MP), the N-HPT analogue which lacks the N−OH group, did not result in cleavage of the RNA (Figure 1, lanes 2 and 5). We also investigated whether N-HPT photoproducts give rise to RNA cleavage. We repeated the photolysis reactions of N-HPT (1 mM) in the absence of RNA, adding the RNA after 5 min of photolysis, in the dark (Figure 1, lane 4). No detectable RNA cleavage resulted under these conditions, suggesting that the photoproducts of N-HPT are not responsible for the observed cleavage. N-HPT-induced RNA cleavage occurred at nucleotide resolution as evidenced by comparison with the RNA cleavage pattern produced by incubation of the RNA with the hydroxyl radical source, peroxynitrous acid (Figure 1, lane 6).

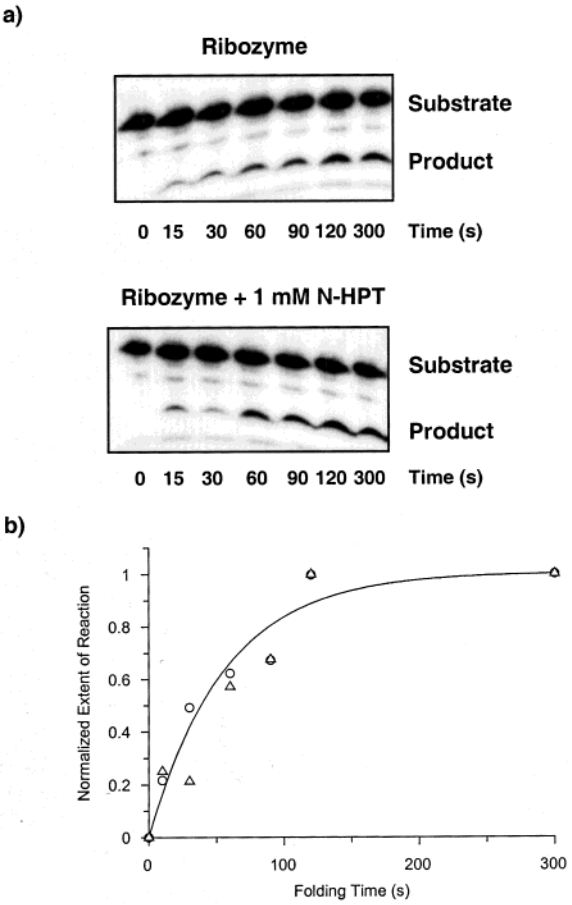

FIGURE 2: Measurement of the endoribonuclease activity as a function of time following addition of Mg^{2+}. (a) Denaturing PAGE analysis of ^{32}P-labeled substrate cleavage in the absence and presence of 1 mM N-HPT. (b) Plot of normalized extent of reaction vs folding time. The observed activity is proportional to the amount of folded ribozyme. Circles (○) are data collected in the absence of N-HPT, and triangles (△) are data collected in the presence of 1 mM N-HPT. With or without N-HPT, the folding rate, k_f, is 0.018 ± 0.003 s^{-1}.

Folding Rates of the Ribozyme. We were interested in examining the effects, if any, of incubation of N-HPT on RNA folding, structure, and function. The overall folding rate of the *Tetrahymena* ribozyme in the presence of N-HPT was measured utilizing the ribozyme's endoribonuclease activity (*26*). The activity assay involves measuring the extent of the ribozyme-catalyzed reaction between GTP and an 11 nucleotide ^{32}P-labeled RNA substrate (eq 3; Figure 2a) as a function of time following initiation of RNA folding with Mg^{2+}. The folding rate was found to be identical to the rate of folding in the absence of N-HPT (Figure 2b); the extents of reaction for the same folding times were identical with or without N-HPT.

$$^{32}\text{P-CCCUCUAAAAA} + \text{GTP} \xrightarrow[Mg^{2+}]{\textit{Tetrahymena}\ \text{ribozyme}} {}^{32}\text{P-CCCUCU} + \text{pppGAAAAA} \quad (3)$$

In addition, the characteristic footprint pattern produced by peroxynitrous acid treatment of the folded RNA (*9,10*) was not affected by the presence or absence of N-HPT (data not shown).

RNA Footprinting by Photolysis of N-HPT. N-HPT was tested as an RNA footprinting reagent by examining its photochemistry in the presence of the unfolded and folded forms of the *Tetrahymena* RNA. Photolysis of buffered solutions of N-HPT in the presence of ^{32}P-labeled *Tetrahymena* RNA resulted in sequence-independent cleavage of the RNA as monitored by denaturing PAGE (Figure 3, lane 3). We then prepared solutions of the RNA, N-HPT, and buffer which also contained 10 mM Mg^{2+}. These were incubated at room temperature for 10 min to allow the RNA to fully fold and were then irradiated at 350 nm for 5 min. Analysis by denaturing PAGE again showed that RNA cleavage occurred but with visible areas of protection (Figure 3, lane 4). These footprints were mapped by comparison with an RNase T1 G cleavage ladder (Figure 3, lane 1) and found to correspond to areas protected from hydroxyl radical cleavage effected by iron-EDTA, synchrotron X-ray irradiation (*8*), or treatment with peroxynitrous acid (Figure 3, lane 5; *9, 10*). The two most prominent footprints correspond to the P3 and P4 regions of the *Tetrahymena* intron—protections of ~50% relative to the unfolded RNA were observed for these regions. Additional regions of protection, corresponding to those seen in footprinting experiments performed with iron-EDTA, X-ray-generated hydroxyl radicals, and peroxynitrous acid (*5, 8*−*10*), were also observed (data not shown).

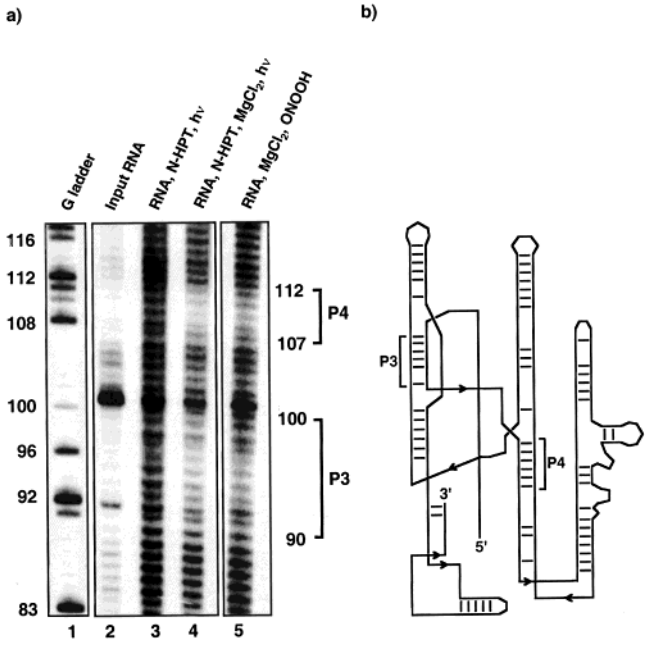

FIGURE 3: (a) Portion of denaturing PAGE analysis of photochemical footprinting of the *Tetrahymena* L-21 ribozyme. Lane 1: RNase T1 G ladder. Lane 2: Input RNA. Lane 3: Cleavage of unfolded ribozyme by N-HPT photolysis (350 nm, 5 min). Lane 4: Cleavage of folded ribozyme by N-HPT photolysis (350 nm, 5 min). Lane 5: Cleavage of folded ribozyme using peroxynitrous acid. (b) Secondary structure of the ribozyme with the P3 and P4 helical regions underlined.

DISCUSSION

We investigated the RNA cleavage properties of radicals from the photolysis of N-HPT in the presence of the 385 nucleotide ^{32}P-labeled *Tetrahymena* RNA. We chose the *Tetrahymena* RNA for these studies because it has been extremely well characterized both biochemically and by X-ray crystallography (*27, 28*). As well, hydroxyl radical footprinting studies have been performed on this molecule using iron-EDTA, synchrotron X-ray irradiation (*8*), and peroxynitrous acid (*9, 10*) as hydroxyl radical sources. Thus, the hydroxyl radical cleavage pattern for this RNA is well established and has been correlated to a large extent with high-resolution structural information.

The *Tetrahymena* RNA has a secondary structure consisting of single-stranded and double-stranded regions and folds into its active conformation in the presence of Mg^{2+} (Figure 3b). Our initial experiments with N-HPT as a photochemical radical source were carried out in the presence of unfolded RNA in order to assess the extent and sequence dependence of any observed cleavages. Photolysis of N-HPT in the presence of ^{32}P-labeled *Tetrahymena* RNA resulted in RNA cleavage as assayed by denaturing PAGE (Figure 1). This cleavage occurred with nucleotide resolution and was independent of sequence. In addition, double-stranded regions of RNA were cleaved as efficiently as single-stranded regions. Cleavage of the RNA was absolutely dependent on both irradiation and the presence of the *N*-hydroxy functionality. The cleavage pattern observed in the experiments with N-HPT was essentially identical to that generated by treatment of the same RNA with peroxynitrous acid as the hydroxyl radical source. These observations, combined with the known photochemistry of N-HPT, suggest it acts as a source of hydroxyl radicals which initiate a reaction cascade leading to cleavage of the phosphodiester backbone.

Redmond and co-workers have reported that laser photolysis of aqueous solutions of N-HPT at 355 nm produced hydroxyl radicals with quantum yields of 12−24% as determined by reaction of the hydroxyl radical with thiocyanate (*23*). We investigated the steady-state photolysis of dilute (1 mM) solutions of N-HPT and found that 5 min of irradiation with a lamp at 350 nm was sufficient to convert most of the N-HPT to products. Based on results with peroxynitrous acid in which ~10% yield of hydroxyl radical (*29*) from 2−5 mM solutions allowed footprinting of the *Tetrahymena* RNA, we reasoned that 1 mM solutions of N-HPT might serve as a photochemical source of radicals for RNA footprinting. N-HPT generates several reactive intermediates upon photolysis in neutral aqueous solutions where N-HPT is largely ionized (Scheme 1; *23*). They include the 2-pyridylthiyl radicals, the *N*-oxy-2-pyridylthiyl radicals, and a solvated electron (the latter two occurring as a result of photoionization with $\Phi_{e^-} = 0.05$ at 355 nm) in addition to hydroxyl radicals (*23*). It is possible that the pyridylthiyl radicals may initiate RNA cleavage during our reactions. However, since the cleavage patterns and footprints are essentially identical to those produced from other hydroxyl radical sources, any competing processes leading to RNA cleavage are indistinguishable and therefore ir-

relevant in terms of N-HPT's utility as a photochemical footprinting reagent.

We carried out photolysis experiments with N-HPT in the presence of folded *Tetrahymena* RNA in order to assess whether footprints corresponding to the folded structure could be observed (Figure 3). A number of protected regions were observed when these reactions were analyzed by denaturing PAGE. These regions corresponded to those protected from cleavage in experiments performed with iron-EDTA, synchrotron X-ray irradiation, or peroxynitrous acid (*5, 8*−*10*). Strong footprints, corresponding to 50−60% protection in comparison with unfolded RNA, were observed for the P3 and P4 regions that are part of the core of the folded *Tetrahymena* RNA. From the endoribonuclease folding assay, we found that the presence of N-HPT does not affect either the folding process or the catalytic activity of the ribozyme (Figure 2). As well, peroxynitrous acid generated footprints are unaffected by the presence of N-HPT, indicating that the N-HPT does not disrupt RNA structure.

The observations reported here show that photolysis of dilute solutions of N-HPT produces reactive species, most likely hydroxyl radicals, which can cleave the phosphodiester backbone of nucleic acids. The cleavage is independent of sequence or the single-stranded or double-stranded nature of the nucleic acid. Dilute solutions of N-HPT do not interact with RNA in such a fashion as to interfere with the folding or activity of the RNA enzyme examined in this study. N-HPT can serve as a probe of RNA structure; specific regions of the folded *Tetrahymena* RNA corresponding to buried domains in the tertiary structure were protected from cleavage upon photolysis of N-HPT.

N-Hydroxypyridine-2(1*H*)-thione (N-HPT) can serve as a general probe for examining RNA structure through RNA footprinting reactions initiated by simple photolysis using a 350 nm light source. RNA footprinting has been widely used as a structural probe, and, recently, kinetic footprinting has been used to study RNA dynamics (*7*−*10*). The thorough laser flash photolysis and photochemical studies of Redmond and co-workers suggest that it should be feasible to generate enough hydroxyl radicals for footprinting during a single pulse from a typical Nd:YAG laser (∼10 ns pulse, ∼10 mJ output; *22*−*24*). This would permit measurement of the rates of RNA dynamics at least 10-fold faster than have been observed with the kinetic footprinting reagent peroxynitrous acid and comparable to those obtained using synchrotron X-ray irradiation.

CONCLUSIONS

Our experiments show that photolysis of dilute buffered solutions of N-HPT in the presence of a large ^{32}P end-labeled RNA, the *Tetrahymena* ribozyme, results in cleavage of the RNA at nucleotide resolution in a sequence-independent fashion. This cleavage occurs in both double-stranded and single-stranded regions of the RNA. In addition, we observe Mg^{2+}-dependent protection of specific regions of the RNA reflecting the folding of the molecule into its active conformation. These results indicate that N-HPT has general utility as a photochemical nucleic acid footprinting reagent and suggest that it may be useful for kinetic footprinting studies.

ACKNOWLEDGMENT

We thank Keith Ingold for helpful discussions at the beginning of this work and Martha Rook and Jamie Williamson for providing the pT7L-21 plasmid.

REFERENCES

1. Dixon, W. J., Hayes, J. J., Levin, J. R., Weidner, M. F., Dombroski, B. A., and Tullius, T. D. (1991) *Methods Enzymol. 208*, 380.
2. Sigman, D. S., Kuwabara, M. D., Chen, C.-H., and Bruice, T. W. (1991) *Methods Enzymol. 208*, 414.
3. Tullius, T. D., and Dombroski, B. A. (1986) *Proc. Natl. Acad. Sci. U.S.A. 83*, 5469.
4. Chen, C.-H. B., and Sigman, D. S. (1988) *J. Am. Chem. Soc. 110*, 6570.
5. Latham, J. A., and Cech, T. R. (1989) *Science 245*, 276.
6. Klassen, N. V. (1987) in *Radiation Chemistry Principles and Applications* (Farhatazis, I., and Rodgers, M. A., Eds.) pp 29−61, VCH Publishers, New York.
7. Sclavi, B., Woodson, S., Sullivan, M., Chance, M. R., and Brenowitz, M. (1997) *J. Mol. Biol. 266*, 144.
8. Sclavi, B., Sullivan, M., Chance, M. R., Brenowitz, M., and Woodson, S. A. (1998) *Science 279*, 1940.
9. Chaulk, S. G., and MacMillan, A. M. (2000) *Angew. Chem., Int. Ed. Engl. 39*, 521.
10. Chaulk, S. G., and MacMillan, A. M. (2000) *Biochemistry 39*, 2.
11. Armitage, B. (1998) *Chem. Rev. 98*, 1171.
12. MacGregor, R. B., Jr. (1992) *Anal. Biochem. 204*, 324.
13. Chow, C. S., and Barton, J. K. (1992) *Methods Enzymol. 212*, 219.
14. Neenhold, H. R., and Rana, T. M. (1995) *Biochemistry 34*, 6303.
15. Chow, C. S., and Barton, J. K. (1992) *Biochemistry 31*, 3534.
16. Chow, C. S., and Barton, J. K. (1990) *J. Am. Chem. Soc. 112*, 2839.
17. Chang, C.-H., and Meares, C. F. (1982) *Biochemistry 21*, 6332.
18. Saito, I., Morii, T., Sugiyama, H., Matsuura, T., Meares, C. F., and Hecht, S. M. (1989) *J. Am. Chem. Soc. 111*, 2307.
19. Saito, I., Takayama, M., Matsuura, T., Matsugo, S., and Kawanishi, S. (1990) *J. Am. Chem. Soc. 112*, 883.
20. Aveline, B. M., Matsugo, S., and Redmond, R. W. (1997) *J. Am. Chem. Soc. 119*, 11785.
21. Sako, M., Nagai, K., and Maki, Y. (1993) *J. Chem. Soc., Chem. Commun.* 750.
22. Aveline, B. M., Kochevar, I. E., and Redmond, R. W. (1996) *J. Am. Chem. Soc. 118*, 10124.
23. Aveline, B. M., Kochevar, I. E., and Redmond, R. W. (1996) *J. Am. Chem. Soc. 118*, 10113.
24. Aveline, B. M., and Redmond, R. W. (1999) *J. Am. Chem. Soc. 121*, 9977.
25. Adam, W., Ballmaier, D., Epe, B., Grimm, G. N., and Saha-Möller, C. R. (1995) *Angew. Chem., Int. Ed. Engl. 34*, 2156.
26. Zarrinkar, P. P., and Williamson, J. R. (1994) *Science 265*, 918.
27. Cate, J. H., Gooding, A. R., Podell, E., Zhou, K., Golden, B. L., Kundrot, C. E., Cech, T. R., and Doudna, J. A. (1996) *Science 273*, 1678.
28. Golden, B. L., Gooding, A. R., Podell, E., and Cech, T. R. (1998) *Science 282*, 259.
29. Richeson, C. E., Mulder, P., Bowry V. W., and Ingold, K. U. (1998) *J. Am. Chem.* Soc. *120*, 7211.

BI0009136